Physics of the Earth and Planetary Interiors, 69 (1991) 72–84
Elsevier Science Publishers B.V., Amsterdam

Constitution of the mantle. 2. Petrological models of transition zone based on FMS phase diagram

O.L. Kuskov, O.B. Fabrichnaya and L.M. Truskinovsky

V.I. Vernadsky Institute of Geochemistry and Analytical Chemistry, USSR Academy of Sciences, Kosygin str. 19, 117334 Moscow, USSR

(Received 9 February 1989; revised and accepted 20 November 1990)

ABSTRACT

Kuskov, O.L., Fabrichnaya, O.B. and Truskinovsky, L.M., 1991. Constitution of the mantle. 2. Petrological models of transition zone based on FMS phase diagram. Phys. Earth Planet. Inter., 69: 72–84.

A detailed picture is presented of phase transformations in the mantle transition zone, based upon the study of phase relations and topologies in the FeO–MgO–SiO_2 (FMS) system. The $(P-T)_x$ diagram for the composition close to pyrolite (SiO_2 = 40 mol.% and Fe/(Fe + Mg) = 0.12) is used in modelling the structure of the mantle transition zone, to connect phase transitions in minerals to the observed seismic discontinuities. The mineralogical nature of the first seismic discontinuity, at a depth of about 400 km, is associated either with a univariant transformation $Px + \alpha + \gamma \rightarrow \alpha + \beta + Px$ or with a sharp divariant transformation $\alpha + Px \rightarrow \alpha + \beta + Px \rightarrow \beta + Px$, which should be closer to 420 km. For the fixed composition close to pyrolite at a depth of about 650 km neither univariant nor invariant equilibria are observed in the FMS system. It has been found that, in the FMS system, two extremely narrow (1–2 km wide) stability fields of divariant mineral assemblages γ + Pv + St and γ + Pv + Mw, separated by a trivariant zone γ + Pv (about 5 km wide) might be responsible for the nature of the 650 km discontinuity. Because of the negative slope of the phase boundaries, the second seismic discontinuity in the cold subducting slab is deeper than in the surrounding mantle.

1. Introduction

In the last decade, studies in experimental petrology, geophysics and geodynamics have focused on the mineral composition and structure of the mantle transition zone, where anomalies in seismic wave velocities, probably caused by phase transformations in the minerals, have been recorded and distinct seismic boundaries, as well as sources of deep-focal earthquakes, have been observed at depths around 400 and 650 km.

The chemical composition of the transition zone is uncertain and has been a matter of intense discussion. Despite the wide acceptance of the pyrolite model of the mantle (Ringwood, 1975; Weidner, 1986; Bina and Wood, 1987; Irifune and Ringwood, 1987; Ito and Takahashi, 1987), it has been suggested (Bass and Anderson, 1984; Anderson and Bass, 1986) that the transition zone is chemically distinct from the upper and lower mantle. The depth of the discontinuity that separates the upper mantle and transition zone is in the range of 390–430 km (Fukao et al., 1982; Grand and Helmberger, 1984; Walck, 1984), and may represent isochemical phase transformations in the olivine plus orthopyroxene components of a pyrolite assemblage or a chemical boundary between pyrolite and piclogite.

Liu (1979), Jeanloz and Thompson (1983), Lees et al. (1983), Bass and Anderson (1984) and Anderson and Bass (1986) have discussed the difficulties of explaining the 670 km discontinuity and velocities in the transition zone on the basis of isochemical phase transformations, and concluded that the 670 km discontinuity may represent a chemical boundary. The depth of the boundary

separating the transition zone and the lower mantle is in the range of 640–720 km (Hales et al., 1980; Vinnik et al., 1983).

According to current concepts, an adequate description of mantle rocks proves to be the system $CaO–FeO–MgO–Al_2O_3–SiO_2$ (CFMAS), the dominant role within the framework of this system belonging to the subsystem $FeO–MgO–SiO_2$ (FMS) which accounts for about 93% of the total chemical composition of the mantle. As thermodynamic data are unavailable and description of solid solutions is complicated for minerals of the CFMAS system, it is impossible to calculate accurately the phase diagram of this system. That is why we have calculated the phase diagram of the simple FMS system, and thermodynamic data on this system should be involved in the data base of the CFMAS system. Some essential features of the phase diagram of the FMS system will be related on phase diagrams for more complex systems. The mineral structure of the mantle based on phase relations in the FMS system is a preliminary result, but an indispensable one for further investigations. Within the limits of research of the FMS system, the 400 km seismic discontinuity may be interpreted as a phase transformation in olivine (Ringwood, 1975; Akaogi and Akimoto, 1979; Navrotsky and Akaogi, 1984; Akimoto, 1987; Bina and Wood, 1987), whereas the seismic discontinuity at 650–670 km may be interpreted in terms of dissociation of γ-spinel into perovskite + magnesiowüstite (Yagi et al., 1979; Ito and Yamada, 1982; Ito et al., 1984; Ito and Takahashi, 1988).

Kuskov and Galimzyanov (1986), Kuskov et al. (1989) and Fabrichnaya and Kuskov (1991) have constructed the complete $P–T$ and $P–T–x$ diagrams of the systems $MgO–SiO_2$ and $MgO–FeO–SiO_2$ within the ranges 10–30 GPa and 1000–2000 K by minimizing Gibbs free energy. The purpose of the present work is to construct the $(P–T)_x$ diagram of the system $FeO–MgO–SiO_2$ with a fixed bulk chemical composition (x) characterizing the petrological model of the Earth's mantle. As demonstrated in the present work, the $(P–T)_x$ diagram of the FMS system is an effective tool for analysing the fine structure of the mantle transition zone and permits us not only to lay down a reliable basis for the existing geophysical models, but also to throw light on some crucial problems of the mantle structure which cannot yet be solved by traditional methods of experimental petrology and seismology.

2. $(P–T)_x$ diagrams of the system $FeO–MgO–SiO_2$

The $P–T–x$ relations in the pseudobinary $Mg_2SiO_4–Fe_2SiO_4$ and $MgSiO_3–FeSiO_3$ systems, calculated by Fabrichnaya and Kuskov (1991), cannot be directly used for modelling the mineral composition of the mantle. To describe its mineral structure we must construct the $P–T$ diagram of the FMS system with a bulk chemical composition typical for the mantle. We shall call such diagrams, $(P–T)_x$ diagrams; they differ from complete $P–T$ diagrams in that the bulk composition of the system (x) is a fixed one.

The $(P–T)_x$ diagram is to be calculated on the basis of isothermal $P–x$ sections for a given SiO_2 content corresponding to the chosen model of mantle composition. For each temperature the succession in the change of phase assemblages with increasing pressure is recording for a fixed Fe/(Fe + Mg) ratio, and the pressure values at the boundaries of divariant regions are projected onto the $P–T$ plane.

Formulae which are used to calculate the Fe/(Fe + Mg) ratio at the conodes interconnecting the compositions of the phases which are in equilibrium for a given SiO_2 content are obtainable from the condition of mass balance. If we let a conode interconnect phases of the olivine and pyroxene composition, then the mass balance of SiO_2 will have the forms

$$\xi^{Px} + \xi^{\alpha} = 1$$

$$\xi^{Px} \cdot \tfrac{1}{2} + \xi^{\alpha} \cdot \tfrac{1}{3} = \mathring{X}_{SiO_2}$$

where the coefficients $\frac{1}{2}$ and $\frac{1}{3}$ are the fractions of SiO_2 in pyroxene and olivine, respectively, and ξ^{α} and ξ^{Px} are the fractions of the bulk mixture composition involved in the formation of the phases α and Px, which are unambiguously determined from the system of equations. The Fe/(Fe + Mg) ratio at the conode interconnecting

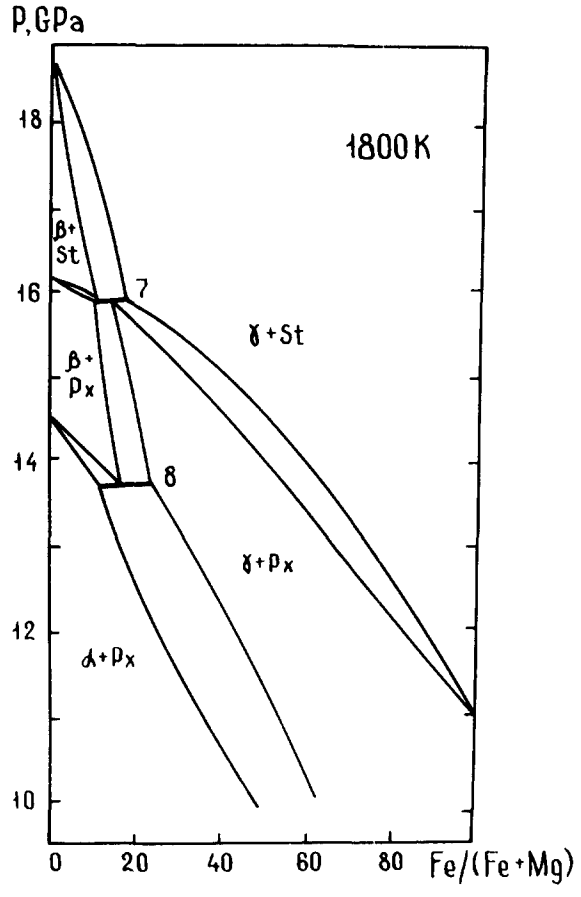

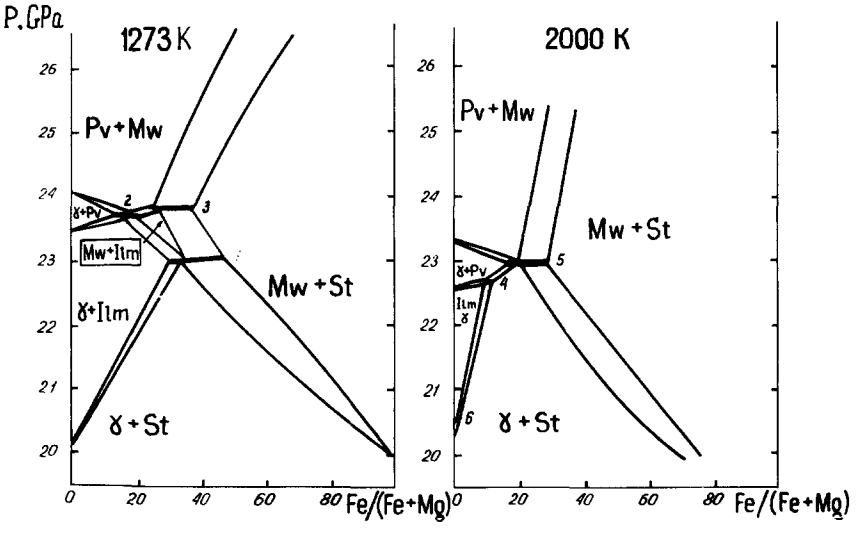

Fig. 1. Phase relations in the FeO–MgO–SiO_2 system within the 10–26 GPa interval according to the Fe/(Fe+Mg) ratio (X_{SiO_2} = 0.4). Figures indicate univariant equilibria: 1, γ + St = Ilm + Mw; 2, γ + Ilm = Pv + Mw; 3, Ilm = Pv + Mw + St; 4, Ilm = Pv + γ + St; 5, γ + St = Pv + Mw; 6, β + St = Ilm + γ; 7, γ + Px = β + St; 8, α + γ = β. a, 10–18 GPa pressures; b, 20–26 GPa pressures.

the phases of olivine and pyroxene composition may be written in the form

$$\frac{\mathrm{Fe}}{\mathrm{Fe}+\mathrm{Mg}} = \frac{\xi^{\mathrm{Px}} X^{\mathrm{Px}}_{\mathrm{FeO}} + \xi^{\alpha} X^{\alpha}_{\mathrm{FeO}}}{1 - \mathring{X}_{\mathrm{SiO_2}}}$$

The FeO fractions in the phases are related to the Fe/(Fe + Mg) value by the following relationships:

$$X^{\alpha}_{\mathrm{FeO}} = \tfrac{2}{3} X^{\alpha}_{\mathrm{Fe_2SiO_4}},\quad X^{\mathrm{Px}}_{\mathrm{FeO}} = \tfrac{1}{2} X^{\mathrm{Px}}_{\mathrm{FeSiO_3}}$$

and the final formula can be rewritten in the form

$$\frac{\mathrm{Fe}}{\mathrm{Fe}+\mathrm{Mg}} = \frac{\xi^{\mathrm{Px}} \tfrac{1}{2} X^{\mathrm{Px}}_{\mathrm{FeSiO_3}} + \xi^{\alpha} \tfrac{2}{3} X^{\alpha}_{\mathrm{Fe_2SiO_4}}}{1 - \mathring{X}_{\mathrm{SiO_2}}} \qquad (1)$$

If a conode connects the phase of pyroxene composition and magnesiowüstite, the Fe/(Fe + Mg) ratio at the conode is determined from the formula

$$\frac{\mathrm{Fe}}{\mathrm{Fe}+\mathrm{Mg}} = \frac{\xi^{\mathrm{Px}} \tfrac{1}{2} X^{\mathrm{Px}}_{\mathrm{FeSiO_3}} + \xi^{\mathrm{Mw}} X^{\mathrm{Mw}}_{\mathrm{FeO}}}{1 - \mathring{X}_{\mathrm{SiO_2}}} \qquad (2)$$

Similarly, it can be shown that the Fe/(Fe + Mg) ratio at the conode connecting SiO_2 and a variable-composition phase is equal to Fe/(Fe + Mg) in the variable-composition phase.

As seen from the formulae (1) and (2), the Fe/(Fe + Mg) ratio at the conodes represents a linear combination of the Fe/(Fe + Mg) ratios of the connected phases. Thus, given a complete phase diagram of the system, we can plot the $(P-T)_x$ diagrams of the system with a different

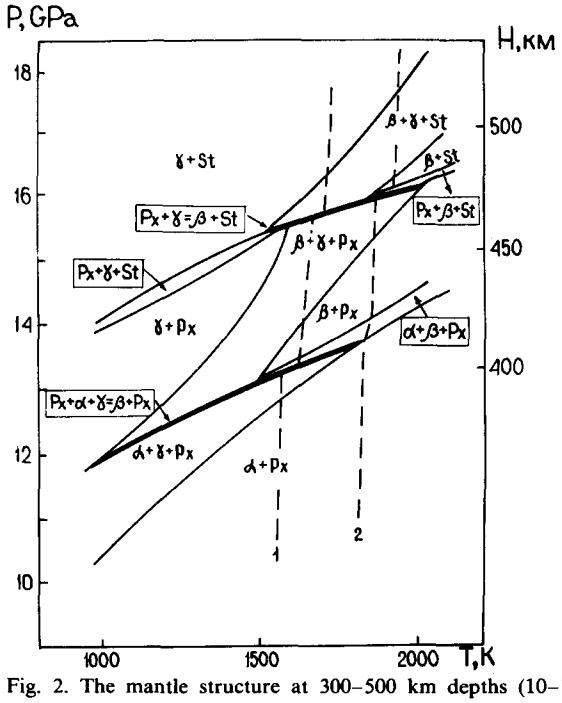

Fig. 2. The mantle structure at 300–500 km depths (10–17 GPa) according to data on phase relations in the FeO–MgO–SiO_2 system for a composition close to pyrolite (Si/(Mg + Fe + Si) = 0.4; Fe/(Fe + Mg) = 0.12). Dashed lines indicate schematically the adiabatic distribution of temperature in the mantle: 1, T_0 (400 km) = 1600 K; 2, T_0 (420 km) = 1820 K; along the univariant curves of phase transformations at 400 and 460 km depths (thick lines) a sharp variation in temperature occurs.

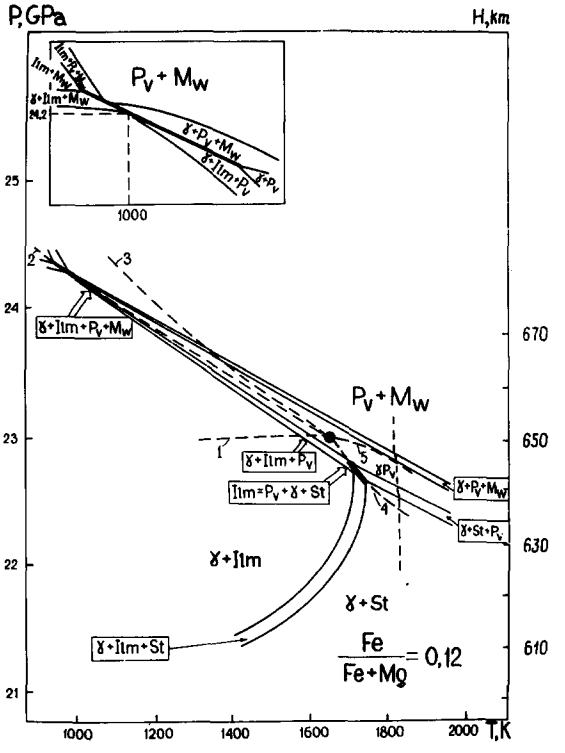

Fig. 3. The mantle structure at 600–700 km depth (21–25 GPa) according to data on phase relations in the FeO–MgO–SiO_2 system for a composition close to pyrolite (see Fig. 2). Dashed line indicates the adiabatic distribution of temperature, which has a negative gradient in the divariant zones of the coexisting solid solutions (γ + St + Pv) and (γ + Pv + Mw) at about 640 and about 650 km depths. A segment of the univariant reaction Ilm = Pv + γ + St in the vicinity of 23 GPa and 1700 K is made prominent by a thick line. Shown in the inset is a univariant reaction γ + Ilm = Pv + Mw, made prominent by a thick line.

bulk composition, corresponding to different models of mantle composition. From a comparison of bulk modulus and bulk sound velocity profiles for the upper mantle, it is concluded that mixtures of olivine + pyroxene with X_{SiO_2} less than 0.36 are inadequate (Kuskov and Panferov, 1991). The likely bulk chemical composition for the upper mantle with X_{SiO_2} of 0.4 and Fe/(Fe + Mg) of 0.12 (which is close to the peridotite or pyrolite composition) has been chosen. Phase relations in the FMS system with $X_{SiO_2} = 0.4$ at pressures below and above 20 GPa are shown in Fig. 1. On this basis, the $(P-T)_x$ diagrams with a pyrolite Fe/(Fe + Mg) ratio of 0.12 are plotted in Figs. 2 and 3.

3. The mantle structure at 400–600 km depths

As follows from the $(P-T)_x$ diagram of the FMS system shown in Fig. 2, olivine and pyroxene are stable at $P-T$ values of the upper mantle and transition zone. The stability region of olivine extends, according to temperature, as far as 11.5–14.5 GPa, and that of pyroxene as far as 14–16 GPa. As the first seismic boundary in the mantle is confined to 400–430 km depths (13–14 GPa), it is concluded that, as a rule, the phase transition in olivine ($\alpha + \gamma = \beta$) is responsible for the sharp rise in elastic properties at this boundary (Akaogi and Akimoto, 1979; Jeanloz and Thompson, 1983).

Accordingly, the univariant reaction $\alpha + \gamma = \beta$ can serve as a temperature indicator (geothermometer) for the first seismic boundary. If we use the $\alpha = \beta$ transformation in pure Mg_2SiO_4 for this purpose, then at 400 km depth the temperature will be 1400 K (Kuskov et al., 1989). This value should be regarded as the lower temperature limit for this depth. A univariant transformation $\alpha + \gamma = \beta$ in the FMS system marks a higher temperature level at the depth of the first seismic boundary, equal to about 1600 K. For this temperature, and at fixed bulk composition, the phase reaction proceeding at 400 km depth can be written in the form of an equation, in which pyroxene takes part as an indifferent phase:

Px + α-olivine + γ-spinel
= β-spinel + α-olivine + Px

reflecting the physico-chemical nature of the first seismic boundary (Kuskov and Fabrichnaya, 1987).

It should be noted that up to 1800 K these phase changes in the FMS system correspond to the phase changes $\alpha + \gamma \rightarrow \alpha + \beta$ in the work of Akaogi and Akimoto (1979) and Navrotsky and Akaogi (1984) rather than the change $\alpha \rightarrow \alpha + \beta$ in the recent results of Katsura and Ito (1988) and Akaogi et al. (1991) for the olivine system.

As, according to seismic data, the boundary has a thickness in the range of 5–15 km (Fukao et al., 1982), sharp changes in physical properties along the boundary are associated, as a rule, with a univariant transformation in olivine. For the chosen pyrolitic composition this allows us to establish the upper temperature limit at 400 km depth as 1820 K—at higher temperatures the univariant curve $\alpha + \gamma = \beta$ disappears on the $(P-T)_x$ diagram (Fig. 2), which is in agreement with results of Katsura and Ito (1988) and Akaogi et al. (1991).

However, calculations have indicated that an interpretation of the nature of the 400 km boundary within the framework of a univariant transformation in the system is not unique. It is found that the mineral nature of this boundary can also be related to a divariant zone $\alpha + \beta$ + Px present at about 420 km depth. A similar view was suggested by Bina and Wood (1987). The divariant zone thickness in the case of an adiabatic distribution of temperature is not more than 10 km and this satisfies Katsura and Ito's (1988) experimental results and seismic criterion for boundary sharpness reasonably well. The minimum temperature at 420 km depth is then 1820 K.

The above discussion indicates that because of: (1) reported uncertainty in the position of the boundary (400–420 km); (2) errors in the thermodynamic information used, leading to a $\pm$ 1 GPa error in pressure of phase transition; and (3) an insignificant slope of the univariant curve Px + α + $\gamma = \beta$ + Px ($dP/dT \approx 30 \times 10^{-4}$ GPa deg^{-1}), the temperature at the depth of the first seismic boundary may vary within a wide range from about 1600 to 1820 K and higher.

Thus the answer to the very important question of the nature of the transformation at the depth of the first seismic discontinuity may be an alterna-

tive one: either a univariant or a divariant transformation is responsible for jumps in elastic properties and density. However, we may also examine a possible combination of the two transformations, which is justifiable in the light of current tectonic concepts of ascending (hot) and descending (cold) convective flows in the mantle.

It can then be found that, because of differences in the temperature regime of the mantle, the geophysical boundary can be described by two different phase transformations. In the hot ascending flow there will take place either a univariant transformation olivine + γ-spinel + pyroxene → olivine + β-spinel + pyroxene at 1600–1800 K or a divariant transformation olivine + β-spinel + pyroxene, marking a boundary with an average depth of 420 km ($T \gtrsim 1820$ K). In the cold descending flow ($T \lesssim 1273$ K) there will take place a univariant transformation olivine + γ-spinel + pyroxene → β-spinel + γ-spinel + pyroxene, which is responsible for jumps in elastic properties at a boundary with an average depth of 380 km. However, as follows from the phase diagram in Fig. 2, the above-mentioned univariant reaction does not exist at temperatures lower than 1000 K and the divariant reaction $\alpha + \gamma + \mathrm{Px} \rightarrow \gamma + \mathrm{Px}$, accompanied by slight volume effect, takes place. In this case, the sharp discontinuity separating the uppermost mantle and the transition zone in the normal mantle might not appear in the cold descending slab.

Such an assumption finds support, to a certain extent, in regional seismic observations in the last decade, according to which the depth of the boundary has a 'floating' character and velocity jumps are recorded at 400, 411 and 430 km depths (Hales et al., 1980; Dziewonski and Anderson, 1981; Fukao et al., 1982; Grand and Helmberger, 1984; Walck, 1984).

According to Bolt (1984), on a particularly distinct seismogram, of an explosion at Novaya Zemlya, peaks are absent in the interval between the phases P′650P′ and P′80P′, which should have been expected if an abrupt reflecting surface were present at an intermediate depth (say, 400 km). The absence of peaks, according to Bolt, is an indication that either sharp discontinuities are absent underneath the Antarctic or they could not be detected with the aid of short-period P-waves because of the less abrupt character of these boundaries as compared with the 650 km discontinuity.

At 400–500 km depth within the temperature range 1600–1800 K, the divariant reactions $\beta + \mathrm{Px} \rightarrow \beta + \gamma + \mathrm{Px}$ and $\beta + \gamma + \mathrm{St} \rightarrow \gamma + \mathrm{St}$ occur, accompanied by slight volume effects.

At 460–470 km depth a univariant reaction pyroxene + γ-spinel = β-phase + stishovite, accompanied by a marked change in density, takes place. The existence of a boundary at about 500 km depth appears to be controversial as yet. However, Hales et al. (1980) identified underneath the Australian continent a boundary at 512 km depth, where the velocity of longitudinal waves increases by 2% (from 9.40 to 9.57 km s^{-1}). However, its nature may be associated not with the reaction $\mathrm{Px} + \gamma = \beta + \mathrm{St}$ in the FMS ternary system, but rather with a pyroxene–garnet transformation in the MAS or CFMAS system at about 500 km depth (Akaogi and Akimoto, 1977; Liu, 1977). On the other hand, Akaogi et al. (1987) indicated that the bulk sound velocity of the pyroxene–garnet system increases very gradually with depth, without any sharp velocity change, because of the gradual dissolution of pyroxene in garnet.

For the FMS system with composition close to pyrolite, the succession of phase transformation at 400–600 km depths along two adiabats is as follows (Fig. 2):

$T(400\ \mathrm{km}) = 1600\ \mathrm{K}$

$$\alpha + \mathrm{Px} \rightarrow \alpha + \gamma + \mathrm{Px} \xrightarrow{400\ \mathrm{km}} \alpha + \beta + \mathrm{Px} \rightarrow \beta + \mathrm{Px} \rightarrow \beta + \gamma + \mathrm{Px} \xrightarrow{460\ \mathrm{km}} \beta + \gamma + \mathrm{St} \rightarrow \gamma + \mathrm{St}$$

$X^{\mathrm{Px}} = 0.06,\ X^{\alpha} = 0.09,\ X^{\beta} = 0.14,\ X^{\gamma} = 0.24$

$T(420\ \mathrm{km}) = 1820\ \mathrm{K}$

$$\alpha + \mathrm{Px} \xrightarrow{420\ \mathrm{km}} \alpha + \beta + \mathrm{Px} \rightarrow \beta + \mathrm{Px} \rightarrow \beta + \gamma + \mathrm{Px} \xrightarrow{470\ \mathrm{km}} \beta + \mathrm{Px} + \mathrm{St} \rightarrow \beta + \mathrm{St} \rightarrow \beta + \gamma + \mathrm{St} \rightarrow \gamma + \mathrm{St}$$

$X^{\mathrm{Px}} = 0.09,\ X^{\alpha} = 0.12,\ X^{\beta} = 0.17$

where X is the Fe/(Fe + Mg) ratio in the phases participating in the univariant equilibrium $\mathrm{Px} + \alpha$

$+ \gamma = Px + \alpha + \beta$ and the divariant loop $\alpha + \beta +$ Px.

4. The mantle structure at 600–700 km depths

The $(P-T)_x$ diagram of the FMS system for a composition close to pyrolite at pressures of more than 20 GPa is shown in Fig. 3. It is constructed on the basis of $P-x$ diagrams of the FMS system (see Fig. 1b) with fixed SiO_2 content (40 mol.%) and Fe/(Fe + Mg) ratio of 0.12 in the range of 1000–2000 K and 21–25 GPa.

The stability region of the trivariant assemblage γ-spinel + stishovite extends from 16–18 GPa to 22.6–22.2 GPa within the temperature range 1700–2000 K. The univariant reaction γ + Pv + St = Ilm for an Fe/(Fe + Mg) ratio of 0.12 is apparent only within a very narrow temperature range close to 1700 K and 22.8 GPa (see Fig. 3). At higher temperatures this reaction occurs at lower values of Fe/(Fe + Mg). Thus, for instance, at 2000 K the reaction γ + Pv + St = Ilm takes place when the Fe/(Fe + Mg) ratio is 0.1 or less (Fig. 1b), thus underlying an extreme correlation between the concentration of iron in the mantle, phase composition and temperature regime. If the geotherm is passing near 1700 K, for the given Fe/(Fe + Mg) ratio of 0.12, the seismic discontinuity at 640 km depth is likely to be associated with the univariant reaction γ + Pv + St = Ilm.

If the temperature at 600–650 km depth exceeds 1700 K, the second seismic boundary must consist of two different reactions. As seen from Fig. 3, the discontinuity between the transition zone and the lower mantle may be associated with two divariant transformations which occur at temperatures greater than 1700 K:

$$\gamma + St \rightarrow \gamma + St + Pv \rightarrow \gamma + Pv \rightarrow \gamma + Pv + Mw \rightarrow Pv + Mw$$

$$X^{\gamma} = 0.12 \qquad X^{Pv} = 0.1 \qquad X^{Pv} = 0.09$$

$$X^{\gamma} = 0.13 \qquad X^{Mw} = 0.18$$

where X is the Fe/(Fe + Mg) ratio in the phases participating in trivariant equilibria γ + St, γ + Pv and Pv + Mw. The compositions of Pv and Mw phases are in reasonable agreement with those obtained by Ito and Takahashi (1988): $X^{Pv} = 0.04$ and $X^{Mw} = 0.24$.

The stability regions of both divariant assemblages (γ + St + Pv) and (γ + Pv + Mw) are very narrow (about 1 km) and for this reason cannot be identified separately on seismograms, but are recorded only in the form of a single sharp boundary. It should be noted that the calculated width of the γ + Pv + Mw transition is consistent with the recent experimental results of Ito and Takahashi (1988), which demonstrated that γ-spinel dissociates into perovskite and magnesiowüstite within an extremely narrow pressure interval (0.15 GPa at 1873 K).

The depth of the discontinuity between the transition zone and the lower mantle has not been accurately established. The available estimates cover the interval from 640 to 720 km (Hales et al., 1980; Dziewonski and Anderson, 1981; Vinnik et al., 1983; Grand and Helmberger, 1984; Walck, 1984). The reason for such uncertainty seems to be associated not with errors in seismic experiments, but rather with lateral differences in the temperature regime and different phase transitions at a single mantle depth.

Lateral temperature variations in the mantle (in the ascending and descending flows) may attain several hundred degrees and induce variations of up to 20–50 km in the depth of the second seismic boundary. From the geochemical interpretation of the geophysical boundary we may conclude that the regional depth of the discontinuity should have a floating character (see Fig. 3).

If the temperature in the subducting lithospheric plate is about 1000 K, the seismic boundary, as follows from Fig. 3, must lie at 680 km depth (24.2 GPa) and its mineral nature will be determined by a single sharp univariant reaction γ-spinel + ilmenite = perovskite + magnesiowüstite (see inset in Fig. 3). If the mean temperature of the plate is 1400 K, then the seismic discontinuity becomes split into two and lies at 660–664 km depth (23.4–23.6 GPa). The effective width of two divariant (γ + Pv + Mw, γ + Ilm + Pv) and trivariant (γ + Pv) zones of phase transformations is 4 km. This result agrees with data of Richards (1972), who argued that the wave velocity must change within a region less than about 4

km thick to satisfy the observed amplitudes of P′dP′.

In the surrounding mantle, with a mean temperature of 2000 K, the seismic discontinuity splits into two very narrow divariant zones (γ + St + Pv, γ + Pv + Mw) at 630–640 km depth (22.3–22.6 GPa). Thus, in the subduction zones, the boundary between the transition zone and the lower mantle must be at a greater depth than in the surrounding mantle.

The phase transformations presented in the FMS system may not be directly applicable to the mantle because pyroxene mostly dissolves into the garnet phase at pressures higher than 10 GPa when a certain amount of Al_2O_3 is present (Akaogi and Akimoto, 1977; Kanzaki, 1986; Irifune, 1987). However, it is evident that the dissociation of spinel would be the main cause of the 640 km discontinuity. As the decomposition is completed within a narrow pressure interval (0.3 GPa), it will result in a large increase in density and elastic properties over a small depth interval. The depth of the sharp discontinuity is in excellent agreement with observations of P-to-SV converted waves by Vinnik et al. (1983).

5. Parameters of petrological models

An analysis of petrological models constructed on the basis of the $(P–T)_x$ diagrams of the systems $MgO–SiO_2$ and $FeO–MgO–SiO_2$ for compositions close to pyrolite has brought to light some phase boundaries of different variance, with which the sharp seismic discontinuities are likely to be associated. To establish a geochemical interpretation for these discontinuities we must know the temperatures in the mantle and the bulk chemical composition, i.e. the petrological model parameters.

The phase diagrams indicate that the nature of the first seismic discontinuity is associated with the olivine = β-phase transformation. If in the $MgO–SiO_2$ system the variance of this transition is equal to unity, then in the FMS system two phase transformations take place at 400–420 km depths: Px + α + γ → α + β + Px (univariant); and Px + α → α + β + Px → β + Px (divariant). Their use as geothermometers will significantly narrow the assessment limits of temperature in the mantle, as determined from indirect data (heat flow, xenoliths, melting points of rocks and minerals), but at the same time the ambiguity with respect to temperature distribution at the first seismic discontinuity still remains.

The other unknown is the bulk chemical composition which significantly affects the $(P–T)_x$ diagram structure. Introducing a small quantity of FeO as an 'impurity' in the binary system $MgO–SiO_2$ accounts for a variation of the stoichiometric system diagram, which leads to splitting of the univariant curves of the binary system and to the formation of divariant regions of a certain width. In other words, univariant lines in the $P–T$ diagram of the system $MgO–SiO_2$ convert into divariant zones in the $(P–T)_x$ diagram of the FMS system, whereas the invariant point of the $MgO–SiO_2$ system converts into a segment of the univariant line in the system with solid solutions (Truskinovsky, 1986; Truskinovsky et al., 1987). As the impurity concentration increases, the $(P–T)_x$ diagram increasingly deviates from the initial $P–T$ diagram of the subsystem. Qualitative topological variations are observed to take place whenever the figurative point characterizing the bulk composition of the mixture passes into the concentration space region corresponding to a nondegenerate invariant assemblage of the FMS system. In this case, the $(P–T)_x$ diagram will comprise segments of univariant curves intersecting at the invariant point.

Let us follow the topological variations of the $(P–T)_x$ diagram of the $FeO–MgO–SiO_2$ system as are observed to take place in the variation of the content of component FeO (Fig. 4). Topological changes of the $(P–T)_x$ diagram demonstrated in Fig. 4 are derived from $P–x$ diagrams of the FMS system with fixed SiO_2 content (40 mol.%) in the range 1000–2000 K and 20–26 GPa (see, for example, the phase diagrams in Fig. 1).

Denoting by X the Fe/(Fe + Mg) ratio, we shall start with the analysis of the subsystem $MgO–SiO_2$ when $X = 0$ (X_{SiO_2} = 40 mol.%). In the pressure interval of interest we shall then have three univariant curves (γ + St = 2Ilm), (Ilm = Pv) and (γ = Pv + MgO), corresponding to the equi-

libria of the stoichiometric phases. With an insignificant increase in the proportion of FeO ($X < 5\%$) the $(P-T)_x$ cross-section of the phase diagram will transform only insignificantly, this being manifested in the 'blurring' of the univariant curves being converted into narrow divariant zones. The divariant zones of the stoichiometric system become trivariant. In the case of $X \approx 12\%$, segments of univariant curves of the ternary system (Ilm = Pv + γ + St) and (γ + Ilm = Pv + Mw) appear at the phase diagram. A nondegenerated invariant point becomes apparent for $18 \leqslant X \leqslant 19\%$ and exists within a limited interval of compositions $X = 19$–30%. Moving from this point there are initially three univariant curves (Ilm = Pv + γ + St), (γ + Ilm = Pv + Mw) and

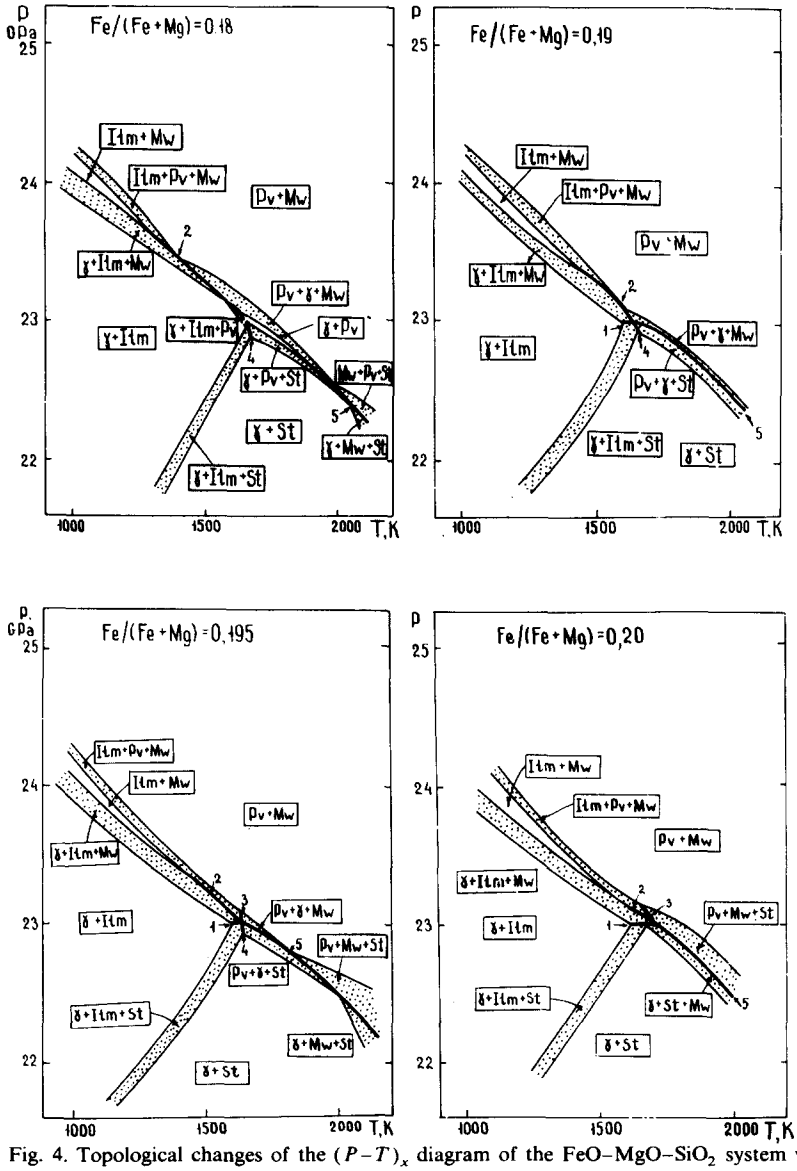

Fig. 4. Topological changes of the $(P-T)_x$ diagram of the FeO–MgO–SiO_2 system with variation in the content of the dissolved component FeO. (For detailed explanations see the text.) Thick lines make prominent the univariant equilibria: 1, γ + St = Ilm + Mw; 2, γ + Ilm = Pv + Mw; 3, Ilm = Pv + Mw + St; 4, Ilm = Pv + γ + St; 5, γ + St = Pv + Mw.

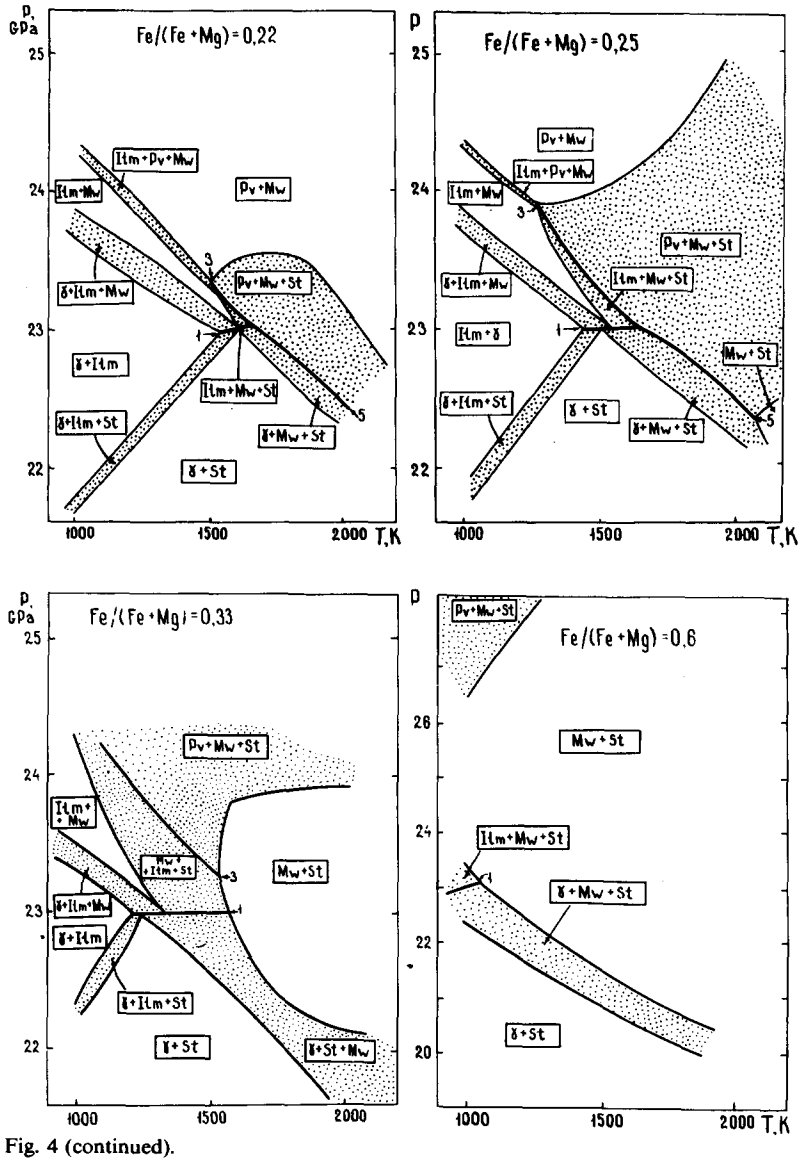

Fig. 4 (continued).

(γ + St = Pv + Mw), and the appearance of the point at $18 \leqslant X \leqslant 19\%$ signifies the disappearance of the trivariant field (γ + Pv). A further insignificant increase in X to 19% leads to the disappearance of the divariant field (Ilm + Pv + γ), but there are now four univariant curves from the invariant point; added to the above-listed three is the equilibrium (γ + St = Ilm + Mw). Transition to $X \approx 19.5$ is accompanied by the immediate disappearance of two divariant fields—(γ + Pv + Mw) and (Pv + γ + St)—and the appearance in their place of the fields (Pv + Mw + St) and (γ + Mw + St). The addition of a further univariant curve occurs at the invariant point: the equilibrium (Ilm = Pv + Mw + St) is added. At $X \approx$ 22% the number of univariant curves in the ternary system begins to decrease. Thus, the equilibria (Ilm = Pv + γ + St) and (Ilm = Pv + Mw + St) disappear but instead of them a new divariant field (Ilm + Mw + St) appears. The nondegener-

ated invariant point disappears at $X \approx 30\%$, and the stability field of oxides opens up in the place of the univariant curve (γ + St = Pv + Mw).

For $X \approx 60\%$, univariant curves are absent within the range of P–T values under discussion, and the pattern of phase relationships is significantly simplified. Approaching the subsystem FeO–SiO_2 ($X \rightarrow 100\%$), narrowing of the remaining divariant regions (Pv, Mw, St) and (γ, St, Mw) occurs and they are changed to univariant curves of the stoichoimetric subsystem. Comparison of the cross-sections shown in Fig. 4 demonstrates the significance of the changes in topologies of the $(P$–$T)_x$ diagram with variation of the Fe/(Fe + Mg) ratio. Thus, for instance, the succession of phase assemblages

$$\gamma + St \rightarrow \gamma + Ilm \rightarrow \gamma + Pv \rightarrow Pv + MgO$$

corresponding to $X \approx 0\%$, converts into a different succession:

$$\gamma + St \rightarrow Mw + St$$

for $X \approx 100\%$. The variety of topologically different $(P$–$T)_x$ phase diagrams is sufficiently large. The effect on the $(P$–$T)_x$ diagram transformations of variation in the Fe/(Fe + Mg) ratio is dependent on the bulk SiO_2 content of the system. All five univariant curves coexist simultaneously in a strictly limited range of Fe/(Fe + Mg) ratio dependent on the SiO_2 content. With the variation of the SiO_2 content between olivine (1/3) and pyroxene (1/2), the maximal changes in topologies take place if the Fe/(Fe + Mg) ratio occurs in the region of the nondegenerated invariant assemblage of the FMS system. However, even for this range of SiO_2 content there are at least four zones which differ as a result of topological transformation. In the range of the SiO_2 content close to olivine, the five univariant curves do not exist simultaneously for any possible Fe/(Fe + Mg) ratio.

The low content of iron in the mantle rocks indicates that the $(P$–$T)_x$ diagrams shown in Figs. 2 and 3 appear to reflect correctly the pattern of phase relationships in the Earth's mantle. At the same time, for Mars, where the Fe content in the rocks may prove to be higher, the fine structure of the mantle will be determined by a different $(P$–$T)_x$ cross-section, in which invariant points insignificant for the Earth's mantle mineralogy may appear.

The study of invariant assemblages is important because the passage of the adiabat through the invariant point is a structurally stable situation; therefore, anomalies of seismic wave velocities may be associated with invariant transformations (Truskinovsky et al., 1985).

6. Conclusions

Thermodynamic simulation seems to be the only approach for determination of a detailed picture of phase equilibria in mineral systems at various P–T–x conditions and to achieve an understanding of the fine structure of the mantle. To understand the chemical composition and mineralogical constitution of the mantle transition zone, phase equilibria in the FeO–MgO–SiO_2 system have been studied in the range of 10–25 GPa and 1000–2000 K. In this paper the following has been concluded.

(1) $(P$–$T)_x$ diagrams of the FMS system for a composition close to pyrolite, with X_{SiO_2} of 0.4 and an Fe/(Fe + Mg) ratio of 0.12, have been calculated, taking into account all known experimental data (phase equilibria and thermochemical).

Topologies of the phase diagrams of the system FeO–MgO–SiO_2 for various Fe/(Fe + Mg) ratios have been examined. The nondegenerated invariant point (Pv + Ilm + γ + St + Mw) discovered at 23 GPa and 1650 ± 100 K exists within the range of Fe/(Fe + Mg) ratios of 0.19–0.30.

(2) It was found that the mineralogical nature of the first seismic discontinuity is associated either with a univariant transformation Px + α + $\gamma \rightarrow \alpha$ + β + Px taking place at about 400 km depth or with a divariant transformation α + Px $\rightarrow \alpha + \beta +$ Px $\rightarrow \beta$ + Px at 420 km depth. In the former case, the mean temperature at 400 km depth is 1600 K; in the latter, the minimal temperature at 420 km depth is 1820 K. According to the phase diagram, the divariant transition is extremely sharp (8–10 km) and is effectively univariant on the scale of the mantle.

(3) The seismic boundary between the transition zone and the lower mantle may be associated with two different divariant transformations occurring at $T \gtrsim 1700$ K; $\gamma + St \rightarrow \gamma + St + Pv \rightarrow \gamma + Pv$ at 630–635 km depth and $\gamma + Pv \rightarrow \gamma + Pv + Mw \rightarrow Pv + Mw$ at 640–645 km depth. Thus, the depth of the discontinuity is close to 640 km, which is 30 km less than in the PREM model, but is in excellent agreement with observations of P-to-SV converted waves by Vinnik et al. (1983).

The stability regions of both divariant assemblages ($\gamma + St + Pv$) and ($\gamma + Pv + Mw$) are very narrow (about 1 km), and for this reason they cannot be separated on seismograms but are recorded only in the form of a single sharp discontinuity.

(4) The depth of the boundary between the transition zone and the lower mantle, as well as the mineral nature of the transition, may vary laterally; in the subduction zones the discontinuity must be sharper and have a greater depth than in the surrounding mantle.

References

Akaogi, M. and Akimoto, S., 1977. Pyroxene–garnet solid solution equilibria in the system $Mg_4Si_4O_{12}$–$Mg_3Al_2Si_3O_{12}$ and $Fe_4Si_4O_{12}$–$Fe_3Al_2Si_3O_{12}$ at high pressures and temperatures. Phys. Earth Planet. Inter., 15: 90–106.

Akaogi, M. and Akimoto, S., 1979. High-pressure phase equilibria in garnet lherzolite, with special reference to Mg^{2+}–Fe^{2+} partitioning among constituent minerals. Phys. Earth Planet. Inter., 19: 31–51.

Akaogi, M., Navrotsky, A., Yagi, T. and Akimoto, S., 1987. Pyroxene–garnet transformation: thermochemistry and elasticity of garnet solid solutions and application to pyrolite mantle. In: M.H. Manghnani and Y. Syono (Editors), High-Pressure Research in Mineral Physics. The Akimoto Volume. Geophysical Monograph 39. Terra, Tokyo, pp. 251–260.

Akaogi, M., Ito, E. and Navrotsky, A., 1989. Olivine–modified spinel–spinel transitions in the system Mg_2SiO_4–Fe_2SiO_4: calorimetric measurements, thermochemical calculation and geophysical application. J. Geophys. Res., 94: 15671–15685.

Akimoto, S., 1987. High-pressure research in geophysics: past, present and future. In: M.H. Manghnani and Y. Syono (Editors), High-Pressure Research in Mineral Physics. The Akimoto Volume. Geophysical Monograph 39. Terra, Tokyo, pp. 1–13.

Anderson, D.L. and Bass, J.D., 1986. Transition region of Earth's upper mantle. Nature, 320: 321–328.

Bass, J.D. and Anderson, D.L., 1984. Composition of upper mantle: geophysical tests of two petrological models. Geophys. Res. Lett., 11: 237–240.

Bina, C. and Wood, B.J., 1987. Olivine–spinel transition: experimental and thermodynamic constraints and implications for the nature of the 400 km seismic discontinuity. J. Geophys. Res., 92: 4853–4866.

Bolt, B.A., 1984. Inside the Earth. Evidence from Earthquakes (Russian translation). Mir, Moscow, 189 pp.

Dziewonski, A. and Anderson, D.L., 1981. Preliminary reference Earth model. Phys. Earth Planet. Inter., 25: 297–356.

Fabrichnaya, O.B. and Kuskov, O.L., 1991. Constitution of the mantle. 1. Phase relations in the FeO–MgO–SiO_2 system at 10–30 GPa. Phys. Earth Planet. Inter., 69: 56–71.

Fukao, J., Nagahashi, T. and Mori, S., 1982. Shear velocity in the mantle transition zone. In: S. Akimoto and M.H. Manghnani (Editors), High-Pressure Research in Geophysics. Center for Academic Publications, Tokyo, pp. 285–300.

Grand, S.P. and Helmberger, D.V., 1984. Upper mantle shear structure of North America. Geophys. J. R. Astron. Soc., 76: 399–438.

Hales, A.L., Muirhead, K.J. and Rynn, J.M.W., 1980. A compressional velocity distribution for the upper mantle. Tectonophysics, 63: 309–348.

Irifune, T., 1987. An experimental investigation of pyroxene–garnet transformation in a pyrolite composition and bearing on the constitution of the mantle. Phys. Earth Planet. Inter., 45: 324–336.

Irifune, T. and Ringwood, A.E., 1987. Phase transformations in primitive MORB and pyrolite compositions to 25 GPa and some geophysical implications. In: M.H. Manghnani and Y. Syono (Editors), High-Pressure Research in Mineral Physics. The Akimoto Volume. Geophysical Monograph 39. Terra, Tokyo, pp. 231–242.

Ito, E. and Takahashi, E., 1987. Ultrahigh-pressure phase transformations and the constitution of the deep mantle. In: M.H. Manghnani and Y. Syono (Editors), High-Pressure Research in Mineral Physics. The Akimoto Volume. Geophysical Monograph 39. Terra, Tokyo, pp. 221–230.

Ito, E. and Takahashi, E., 1988. Post-spinel transformations in the system Mg_2SiO_4–Fe_2SiO_4 and some geophysical implications. Tech. Rep. ISEI, Okayama Univ. Misasa Ser. A, 17: 1–17.

Ito, E. and Yamada, H., 1982. Stability relations of silicate spinels, ilmenites and perovskites. In: S. Akimoto and M.H. Manghnani (Editors), High-Pressure Research in Geophysics. Center for Academic Publications, Tokyo, pp. 405–419.

Ito, E., Takahashi, E. and Matsui, Y., 1984. The mineralogy and chemistry of lower mantle: an implication of the ultrahigh-pressure phase relations in the system MgO–FeO–SiO_2. Earth Planet. Sci. Lett., 67: 238–248.

Jeanloz, R. and Thompson, A.B., 1983. Phase transitions and

mantle discontinuities. Rev. Geophys. Space Phys., 21: 51–74.

Kanzaki, M., 1987. Ultrahigh-pressure phase relations in the system $Mg_4Si_4O_{12}$–$Mg_3Al_2Si_3O_{12}$. Phys. Earth Planet. Inter., 49: 168–175.

Katsura, T. and Ito, E., 1988. The system Mg_2SiO_4–Fe_2SiO_4 at high pressures and temperatures: precise determination of stabilities of olivine, modified spinel. Tech. Rep. ISEI, Okayama Univ. Misasa, Ser. A, 16: 1–15.

Kuskov, O.L. and Fabrichnaya, O.B. 1987. Phase relations in the FeO–MgO–SiO_2 system: the thermodynamic parameters of virtual β-Fe_2SiO_4, and petrological and geophysical applications. Geochem. Int., 24 (9): 56–72.

Kuskov, O.L. and Galimzyanov, R.F., 1986. Thermodynamics of stable mineral assemblages of the mantle transition zone. In: S.K. Saxena (Editor), Chemistry and Physics of Terrestrial Planets. Advances in Physical Geochemistry, Vol. 6. Springer-Verlag, New York, pp. 310–361.

Kuskov, O.L. and Panferov, A.B., 1991. Constitution of the mantle. 3. Density, elastic properties and the mineralogy of the 400 km discontinuity. Phys. Earth Planet Inter., 69: 85–100.

Kuskov, O.L., Fabrichnaya, O.B., Galimzyanov, R.F. and Truskinovsky, L.M., 1989. Computer simulation of the phase diagram for the MgO–SiO_2 system at P–T parameters of the mantle transition zone. Phys. Chem. Minerals, 16: 442–454.

Lees, A., Bukowinski, M. and Jeanloz, R., 1983. Reflection properties of phase transition and compositional change models of 670 km discontinuity. J. Geophys. Res., 88: 8145–8150.

Liu, L., 1977. The system enstatite–pyrope at high pressures and temperatures and mineralogy of the Earth's mantle. Earth Planet. Sci. Lett., 36: 237–245.

Liu, L., 1979. On the 650-km seismic discontinuity. Earth Planet. Sci. Lett., 42: 202–208.

Navrotsky, A. and Akaogi, M., 1984. The α, β, γ phase relations in Fe_2SiO_4–Mg_2SiO_4 and Co_2SiO_4–Mg_2SiO_4: calculation from thermochemical data and geophysical applications. J. Geophys. Res., 89: 10135–10140.

Richards, P.G., 1972. Seismic waves reflected from velocity gradient anomalies within the Earth's upper mantle. Z. Geophys., 38: 517–527.

Ringwood, A.E., 1975. Composition and Petrology of the Earth's Mantle. McGraw–Hill, New York, 618 pp.

Truskinovsky, L.M., 1986. Subsolidus P–T diagrams of multicomponent systems close to stoichiometric ones and the problems of mantle petrology. Geokhimiya, 11: 1535–1549.

Truskinovsky, L.M., Kuskov, O.L. and Khitarov, N.I., 1985. On the stability of invariant points in the mantle transition zone. Dokl. Akad. Nauk SSSR, 285: 83–87 (in Russian).

Truskinovsky, L.M., Fabrichnaya, O.B. and Kuskov, O.L., 1987. On theory of construction of subsolidus P–T diagrams of multicomponent mineral systems. Geokhimiya, 5: 693–712.

Vinnik, L.P., Avetisjan, R.A. and Mikhailova, N.G., 1983. Heterogeneities in the mantle transition zone from observations of P-to-SV converted waves. Phys. Earth Planet. Inter., 33: 149–163.

Walck, M.C., 1984. The P-wave upper mantle structure beneath an active spreading center: the Gulf of California. Geophys. J. R. Astron. Soc., 76: 697–723.

Weidner, D.J., 1986. Mantle model based on measured physical properties of minerals. In: S.K. Saxena (Editor), Chemistry and Physics of Terrestrial Planets. Advances in Physical Geochemistry, Vol. 6. Springer-Verlag, New York, pp. 251–274.

Yagi, T., Bell, P.M. and Mao, H.K., 1979. Phase relations in the system MgO–FeO–SiO_2 between 150 and 700 kbar at 1000 °C. Carnegie Inst. Washington Yearbook, 78: 614–618.